

# Rhomb-I, a P-I metalloproteinase from *Lachesis muta rhombeata* venom degrades vessel extra cellular matrix components and impairs platelet aggregation

Valéria Gonçalves de Alvarenga<sup>a</sup>, Luciana S. Oliveira<sup>a</sup>, Gustavo O. Santos<sup>a</sup>, Dan E. Vivas-Ruiz<sup>b</sup>, Márcia Helena Borges<sup>c</sup>, Rodrigo C.G. de Souza<sup>d</sup>, Johannes A. Eble<sup>e</sup>, Ana Maria Moura-da-Silva<sup>f</sup>, Eladio F. Sanchez<sup>a,\*</sup>

<sup>a</sup> Laboratório de Bioquímica de Proteínas de Venenos Animais, Fundação Ezequiel Dias, Belo Horizonte, Brazil

<sup>b</sup> Laboratório de Biología Molecular, Facultad de Ciencias Biológicas, Universidad Nacional Mayor de San Marcos, Lima, Peru

<sup>c</sup> Laboratório de Proteômica e Aracnídeos, Fundação Ezequiel Dias, Belo Horizonte, Brazil

<sup>d</sup> Serra Grande Center, Itacaré, Bahia, Brazil

<sup>e</sup> Institute of Physiological Chemistry and Pathobiochemistry, University of Münster, Germany

<sup>f</sup> Laboratório de Imunopatologia, Instituto Butantan, São Paulo, Brazil

## ARTICLE INFO

Handling Editor: Ray Norton

### Keywords:

*Lachesis muta rhombeata*  
Snake venom metalloproteinase  
Platelet receptors  
Hemostasis  
Hemorrhage

## ABSTRACT

Rhomb-I, a 23-kDa metalloproteinase was isolated from *L. m. rhombeata* venom. Its dimethylcasein proteolysis was abolished by metal chelators, and slightly enhanced by  $\text{Ca}^{2+}$  and  $\text{Mg}^{2+}$  ions, but inhibited by  $\text{Co}^{2+}$ ,  $\text{Zn}^{2+}$  and  $\alpha 2$ -macroglobulin. In aqueous solution, rhomb-I autoproteolyzed to a 20- and 11-kDa fragments at 37 °C. The amino acid sequence showed high homology with other snake venom metalloproteinases. Rhomb-I causes hemorrhage that may be ascribed to hydrolysis of essential basement membrane, extracellular matrix and plasma proteins. It preferentially cleaves the  $\alpha$ -chains of fibrin (ogen). Rhomb-I inhibited convulxin- and von Willebrand factor (vWF)-induced aggregation on human platelets without significant effect on collagen-stimulated aggregation or other effectors. It digests vWF into a low-molecular-mass multimers of vWF and a rvWF-A1 domain to a 27-kDa fragment as revealed by western blotting with mouse anti-rvWF A1-domain IgG. Incubation of platelets with rhomb-I resulted in adhesion to and cleavage of platelet receptors glycoprotein (GP)Ib $\alpha$  and GPVI to release a 55-kDa soluble form. Both membrane glycoproteins GPIb $\alpha$  that binds vWF, together with GPVI which binds collagen, play a key role in mediating platelet adhesion/activation and can initiate (patho)physiological thrombus formation. Conclusions: rhomb-I is implicated in the pathophysiology of *Lachesis* envenoming by disrupting vasculature, hemostasis and platelet aggregation through impairing vWF-GPIb axis and blocking GPVI-collagen binding.

## 1. Introduction

Snakebite envenoming represents a danger to human health and is a neglected disease worldwide, particularly throughout tropical and sub-tropical countries (Chippaux, 2017; Slagboom et al., 2017). On the other hand, snake venoms are a goldmine of active compounds responsible for the multi-functional activities that perturb vital physiological systems including enzymes, receptors or ion channels, and can be broadly

classified as haemotoxic, neurotoxic or cytotoxic (Vetter et al., 2011; Slagboom et al., 2017). In South America, the predominant group of venomous pitvipers (Crotalinae subfamily of Viperidae) of medical relevance includes the genera *Bothrops*, *Crotalus* and *Lachesis* (Campbell and Lamar, 2004; Chippaux, 2017; Slagboom et al., 2017). Of particular interest, *Lachesis* (bushmaster) inhabits lowland tropical forested areas in Central and South America, is a terrestrial and nocturnal snake, and is the only neo-tropical snake that lays eggs.

**Abbreviations:** ADAM, a disintegrin and metalloproteinase; BM, basement membrane; DMC, dimethylcasein; EDTA, ethylenediaminetetraacetic acid; ECM, extracellular matrix; Fg, fibrinogen; Fb, fibrin; FN, fibronectin; PMSF, phenyl methyl sulfonyl fluoride; ND, nidogen; SVMPs, Snake venom metalloproteinases; vWF, von Willebrand factor; VT, vitronectin.

\* Corresponding author. Research and Development Directory, Ezequiel Dias Foundation, Belo Horizonte, MG, Brazil.

E-mail address: [eladio.flores@funed.mg.gov.br](mailto:eladio.flores@funed.mg.gov.br) (E.F. Sanchez).

<https://doi.org/10.1016/j.toxicon.2023.107097>

Received 18 January 2023; Received in revised form 21 March 2023; Accepted 22 March 2023

Available online 5 April 2023

0041-0101/© 2023 Elsevier Ltd. All rights reserved.

Lachesis is probably the largest viper in the world, up to 3.5 m (Campbell and Lamar, 2004; Souza et al., 2007). Literature on human envenomings by bushmasters is rare and represents approximately 3% of reported accidents in Brazil. However, in the Amazon, snakebites caused by bushmasters are around 9% (Souza et al., 2007; Chippaux, 2017) and should be considered of a great medical emergency, in part due to the quantity of venom delivered by adult snakes around 300–400 mg/snake (Sanchez et al., 1992; Souza et al., 2007). Envenomation attributed to Lachesis is characterized by immediate local pain and edema within a very short time (within 20 min after the bite), mild hemorrhage at the bite site, and neurotoxic activity. Furthermore, Lachesis venom degrades fibrinogen and prothrombin, provoking disseminated intravascular coagulation with fibrinogen consumption and increased bleeding times. Systemic manifestations such as diarrhea, vomiting, cardiovascular (hypotension), and coagulopathy due to massive hyperfibrinolysis and hemorrhage (Torres et al., 1995; Tanus Jorge et al., 1997; Campbell and Lamar, 2004; Souza et al., 2007) are often associated with human accidents. *L. muta* is mainly distributed in equatorial forest, of South American tropical countries. In accordance with the phylogenetic relationships, two subspecies have been described for *L. muta*: *L. m. muta* mainly inhabits the equatorial Amazon tropical forest east of the Andes; and *L. m. rhombeata* occurs in the Atlantic forest of Brazil from Rio de Janeiro to Ceará State (Campbell and Lamar, 2004; Stephano et al., 2005; Souza et al., 2007; Pla et al., 2013).

In spite of the fact that viperid venoms comprise over 100 protein compounds, they belong to only a few protein families, including those with enzymatic activity: metalloproteinases (SVMPs), serine proteinases (SVSPs), L-amino acid oxidases (LAAOs), phospholipases A<sub>2</sub> (PLA<sub>2</sub>s), hyaluronidases among others; and proteins/peptides without enzymatic effect: disintegrins, C-type lectins, myotoxins, CRISP toxins, proteinase inhibitors, natriuretic peptides, cystatin, and Kunitz-type proteinase inhibitors (Serrano et al., 2005; Sanz et al., 2008; Calvete, 2011; Madrigal et al., 2012). Thus, pathophysiological symptoms and clinical evolution of human bite victims of Lachesis are probably a consequence of the direct effect of a few molecules already reported from *L. muta* venom, principally SVMPs (Estevão-Costa et al., 2000; Sanchez, 2004), SVSPs of the three groups: fibrinogen-clotting enzymes (thrombin-like) (Magalhaes et al., 2003), plasminogen activator (Sanchez et al., 2000, 2006), and kallikrein-like proteinases (Felicori et al., 2003; Weinberg et al., 2004), myotoxic K49 PLA<sub>2</sub>s and basic D49 PLA<sub>2</sub>s (Fuly et al., 2000; Damico et al., 2006), among other active molecules.

Among other efforts to improve the characterization of proteins/toxins of Lachesis venom, a comparison of proteomic analysis of the protein composition of *L. m. rhombeata* (Pla et al., 2013; Wiesel et al., 2019) with those of other Central and South American bushmasters (Sanz et al., 2008; Madrigal et al., 2012), provides clues for correlating venom composition and the pathological effects of envenomation across Lachesis venoms. These studies revealed remarkably similar venom phenotypes comprising seven or eight protein families including the aforementioned molecules. In connection with proteomic analysis, transcriptomic investigations were performed by the generation of expressed sequence tags (ESTs) from the venom glands of *L. muta* (Junqueira-de-Azevedo et al., 2006). The main pathological effects such as hemorrhage, local inflammation, and coagulopathy induced by the majority of viperid venoms are related directly or indirectly to the action of SVMPs. SVMPs are major components in most viperid venoms (>30% of all proteins), e.g. Lachesis, capable of inducing a diverse array of functions and disrupting hemostasis by blocking or triggering several steps of the coagulation cascade and impairing platelet functions of human envenoming victims (Torres et al., 1995; Tanus Jorge et al., 1997; Souza et al., 2007). As a result of the extensive representation in viperid venoms, SVMPs are the principal causes of life-threatening hemorrhagic pathologies detected following viperid snakebites (Casewell et al., 2011, 2013). Evolutionarily, SVMPs seem to have evolved from ADAM (A disintegrin and metalloproteinase) genes (Moura-da-Silva et al., 1996; Fry et al., 2008; Brust et al., 2013) that have been

duplicated near the base of advanced snake (Caenophidia) radiation, prior to the divergence of the Viperidae from most other Caenophidians (Moura-da-Silva et al., 1996; Fry et al., 2008; Brust et al., 2013). In accordance with the structural domains, SVMPs are conventionally classified into three classes: P-I, P-II, and P-III (Fox and Serrano, 2005; Takeda et al., 2006) further divided in several subclasses. The P-I class comprises only a metalloproteinase (MP) domain, P-IIs are those sequentially extended by a disintegrin (Dis) domain, and P-IIIs by a Dis-like and cysteine-rich (Cys-) domains. The P-III class SVMPs share a topological similarity that is homologous to the ectodomain of membrane-anchored ADAMs and with matrix metalloproteinases (MMPs) and are included in the M12 clan (MEROPS database: <http://merops.sanger.ac.uk>) of metalloproteinases also termed to as adamalysins or repolysins (Gomis-Rüth, 2003; Takeda et al., 2006; Takeda, 2016). Moreover, after post-translational modification, the SVMPs can be found in several isoforms in the venoms, either only with the catalytic domain (P-I class) or in combination of the catalytic domain with the Dis domain (P-II class) or with Dis and Cys domains (P-III class) (Takeda, 2016; Moura-da-Silva et al., 2016). P-III SVMPs show a high hemorrhagic effect and also more diverse and specific biological activities than the P-I class.

Snake venom proteins and peptides have extremely diverse pharmacology with a wide range of molecular targets mainly in the cardiovascular and nervous systems. Due to the abundance in venoms, their structural and functional diversity, SVMPs offer amazing potentials for the development of newer bioactive agents for innovative therapeutics to treat various thromboembolic and hemostatic disorders and in diagnosis (Hsu et al., 2008; Vetter et al., 2011; Casewell et al., 2013; Kini and Koh, 2016; Sanchez et al., 2017, 2021). With regard to hemostasis and thrombosis, platelets are endowed with a repertoire of surface receptors that enable them to adhere, activate and aggregate at the sites of tissue damage or infection (Andrews et al., 2007). The engagement of the adhesion receptors regulating pathophysiological thrombus formation, the GPIIb-IX-V complex binds to vWF and other ligands, together with the major collagen receptor GPVI and play a critical role in the initiation of platelet adhesion and activation (Andrews et al., 2007; Vilahur et al., 2018; Grover et al., 2018; Sanchez et al., 2021).

The preliminary characterization of a P-I class SVMP, Lmr-MP from *L. m. rhombeata* venom, has been reported previously (Cordeiro et al., 2018). Searching for fibrinolytic SVMPs that affect hemostasis by disrupting blood coagulation, vasculature and platelet function, we describe the purification of a P-I SVMP termed rhomb-I, and have assessed its effects on basement membrane (BM) components, associated extracellular matrix (ECM), and plasma proteins. Particularly, its action upon platelet aggregation and coagulation cascade was investigated. We have found that rhomb-I binds to and cleaves vWF, and the surface platelet receptors GPIIb and GPVI, resulting in impaired platelet activities. Like other SVMPs, rhomb-I has important implications for envenomed patients as several hemostatic processes and physiological targets can be affected by these enzymes.

## 2. Materials and methods

### 2.1. Venom and animals

Lachesis muta rhombeata venom was kindly donated by Dr. Rodrigo C.G. de Sousa from Serra Grande Center for Lachesis muta Breeding, with Authorization of Instituto do Meio Ambiente e Recursos Hídricos No: 2016.001.002764/INEMA/Lic-02764, Bahia State. Swiss Webster mice (female, 18–22 g) from FUNED were used for in vivo experiments in accordance with the guidelines of the Brazilian College for Animal Experimentation and approved by the local Ethics Committee, Protocol number CEUA/FUNED: June 2019.

## 2.2. Reagents

Bacterial expression and purification of recombinant A1 domain of human vWF (rvWF-A1 domain) was performed as reported (Sanchez et al., 2016). Convulxin (CVX) was purified from South American rattlesnake *Crotalus durissus terrificus* venom as described (Polgár et al., 1997), ADP (A2754), thrombin (112,374), prostaglandin E1 (P5515), fibronectin (F2006), vitronectin (5051), bovine (F8630), and human fibrinogen (F4129) essentially plasminogen free were obtained from Sigma Chemical (St. Louis, MO, USA). Von Willebrand factor (vWF, 681, 300) was from Merck (Darmstadt, Germany), type I collagen (5368) and ristocetin (001226) were from Helena Laboratories (Beaumont, TX, USA). The GPVI polyclonal antibody (AF3627) from human platelets and antihuman CD42b/GPIb $\alpha$  polyclonal antibody (AF4067) were from R&D Systems (Minneapolis, USA). Secondary peroxidase conjugated antibody (A6154) was from Sigma. Protein G peroxidase conjugated (P21041) and the ECL chemiluminescent blotting substrate (32,106) were from Thermo Scientific (Waltham, MA USA). N-glycosidase F (PNGase F-P0704S) was from New England Biolabs (Massachusetts, MA, USA). All other chemicals were of analytical grade.

## 2.3. Purification

The proteinase rhomb-I was isolated from *L. m. rhombeata* venom by a two-step purification procedure with size exclusion chromatography. Lyophilized venom (2400 mg) was dissolved in 8 ml of 0.05 M ammonium acetate buffer (pH 7.3) containing 0.3 M NaCl, and centrifuged at 6000 $\times$ g to remove insoluble material. Step A: the supernatant solution (2160 mg) was loaded onto two Sephacryl S-200 (2.5  $\times$  100 cm) columns in series, equilibrated and eluted with the same buffer. The flow rate was 7 ml/h and fractions were collected at 4 °C. Active fractions (Peak 5) of approximately 25 kDa containing proteolytic and low hemorrhagic activity were pooled, dialyzed against distilled water containing 1 mM CaCl<sub>2</sub> and lyophilized. Step B: fractions of peak 5 (471 mg, 21.82% m/v) still containing impurities was applied to a Sephadex G-50 fine (1.5  $\times$  100 cm) column equilibrated and eluted with 20 mM Hepes buffer, pH 7.5 containing 1 mM CaCl<sub>2</sub> at a flow rate of 6 ml/h at 4 °C. Proteins were monitored at 280 nm. Proteinase activity on dimethylcasein (DMC) and hemorrhagic activity on mice were also assessed and SDS-PAGE was performed on selected fractions according to Laemmli (1970). Aliquot of the peak from the B step was diluted in 1 ml trifluoroacetic acid (0.1% TFA, v/v) and submitted to an HPLC system using a reverse phase column (C4 Vydac, 250  $\times$  4.6 mm). Column was washed with 0.1% TFA and subsequently eluted with a linear gradient of 0–80% acetonitrile (ACN) in 0.1% aqueous TFA at a flow rate of 1 ml/h. The peak was collected for further structural characterization.

## 2.4. Mass spectrometry analysis by MALDI-TOF

The relative molecular mass (Mr) of rhomb-I was determined by matrix-assisted laser desorption ionization time of flight mass spectrometry (MALDI-TOF) according to (Naumann et al., 2011). Spectra were recorded and analyzed using an Autoflex III Smartbean instruments in a linear positive mode controlled by the proprietary COMPASS™ 1.2 as described previously (Naumann et al., 2011). The Mr of the isolated protein was also estimated by SDS-PAGE (12.5% gels) from reducing gels and stained with Coomassie blue 250.

## 2.5. Amino acid sequence determination

To determine its amino acid sequence, rhomb-I (50  $\mu$ g protein) was purified by RP-HPLC and submitted to liquid chromatography-tandem mass spectrometry (LC-MS/MS) by the University of São Paulo BIOMASS-Core Facility for Scientific Research (CEFAP-USP). The sample was then denatured with urea, reduced by triethylphosphine, and alkylated by iodoethanol before treatment with trypsin (0.2  $\mu$ g/ $\mu$ l) at

25 °C, overnight. For the LC-MS/MS, peptide samples were redissolved in 0.1% TFA and analyzed using an EASY-nLC system (Thermo Scientific) coupled to a LTQ-Orbitrap Velos mass spectrometer (Thermo Scientific) according experimental conditions reported recently (Nachtigall et al., 2022).

## 2.6. 3D model of rhomb-I

The theoretical rhomb-I 3D model was predicted by comparative homology modeling (Šali and Blundell, 1993). A BLASTp search was performed to identify appropriated rhomb-I homologue templates. Five templates were selected for modeling: 3GBO (Bothrops moojeni), 1DTH (*Crotalus atrox*), 4AIG (*Crotalus adamanteus*), 4Q1L (Bothrops leucurus) and 1ND1 (Bothrops asper). Modeller v 9.16 (Fiser and Šali, 2003) was used to generate rhomb-I structure in.pdb format. The best model was selected based on the least discrete optimized protein energy (DOPE) and modeller objective function (MOF) scores. Root Mean Square Deviation (RMSD) was calculated using the program VMD v 1.9.2 (Humphrey et al., 1996). Validation analysis was conducted using SAVES Sever (<https://services.mbi.ucla.edu/SAVES/>) which includes PROCHECK WHATCHECK, ERRAT, VERIFY-3D and Ramachandran counter map calculations. Finally, the structure visualization was generated by using the Pymol software (Delano, 2002).

## 2.7. Effects of divalent cations and enzyme inhibitors

Proteolytic activity was tested using DMC as substrate as reported in (Sanchez et al., 2000). Rhomb-I (1  $\mu$ g) was incubated with 10 mM of CaCl<sub>2</sub>, MgCl<sub>2</sub>, BaCl<sub>2</sub>, ZnCl<sub>2</sub> and CoCl<sub>2</sub> in 20 mM Hepes buffer, pH 7.4 for 30 min at 37 °C before proteolytic activity was assayed. In addition, enzymatic activity was challenged with several proteinase inhibitors: batimastat (Bat), marimastat (Mar) (0.5  $\mu$ M each), MMP inhibitor-III (i-MMP-III, ratio of 1:50), iodoacetamide (IAA, 1 mM), ethylenediaminetetracetic acid (EDTA, 5 mM), phenyl methane sulfonyl fluoride (PMSF, 5 mM). To determine the stoichiometry of inhibition of rhomb-I with plasma inhibitor  $\alpha$ 2-macroglobulin ( $\alpha$ 2-M), increasing amounts of  $\alpha$ 2-M (7.9–63  $\mu$ g) were incubated with a fixed concentration of rhomb-I (1  $\mu$ g) in 250- $\mu$ l of 20 mM Hepes buffer, pH 7.4 at 37 °C for 5 min. The molar ratios of  $\alpha$ 2-M: proteinase varied from 0.5 to 2.0. The results of enzyme- $\alpha$ 2-M interaction were analyzed by SDS-PAGE. The residual activity was performed with DMC.

## 2.8. Hemorrhagic activity

To elucidate if rhomb-I induces hemorrhage, the skin assay procedure (Sanchez et al., 1992) was modified in a murine model as follows. Three doses of 10, 25 and 50  $\mu$ g venom or rhomb-I were inoculated subcutaneously into a dorsal shaved skin of three animals (20–22 g)/dose. After 4 h the animals were euthanized, the dorsal skin was removed and the diameter of the hemorrhagic halo on the inner surface of the skin was measured. The minimum hemorrhagic dose (MHD) was defined as the amount of venom or enzyme to produce a hemorrhagic halo 1 cm in diameter. The P-I class SVMs, atroxlysin-I (atr-I, hemorrhagic), mutalysin-II (mut-II, *L.m.muta*) and leucurolysin-a (leuc-a, *B. leucurus*) (non-hemorrhagic) were used as positive and negative controls, respectively.

## 2.9. Autodigestion assay

Protein degradation was observed during isolation (Step B). Thus, to verify autoproteolysis, rhomb-I (5  $\mu$ g) in aqueous solution was incubated at 37 °C for 24 h and then the reaction was terminated by adding sample buffer under reducing conditions. The autodigestion pattern was analyzed on SDS-PAGE (18% gel). Another sample of mut-II (5  $\mu$ g) was electrotransferred to a nitrocellulose membrane. Immunoblots were developed with rabbit anti-mutalysin-II IgG (primary antibody) and

anti-rabbit-IgG antibody conjugated with peroxidase (1:2000 dilution), detected with ECL and visualized by chemiluminescence imaging system ChemiDoc (Bio-Rad, Hercules, CA, USA). Furthermore, autoproteolytic fragments of 20- and 11-kDa separated by SDS-PAGE were subjected to automated in-gel digestion with trypsin followed to sequence analysis by LC-MS/MS.

## 2.10. Test to detect the presence of glycoconjugates in the protein

Samples containing 10 µg of rhomb-I were dissolved in 50 µl of denaturing buffer (0.5% SDS, 1% 2β-ME). The protein was denatured by boiling it for 5 min. After the addition of 20 µl of reaction buffer (50 mM Tris-HCl, pH 8.0), 2.5 µl of detergent solution (IGEPAL 15% Roche), and 2 units of recombinant PNGase F, the samples were incubated for 6 h at 37 °C according to (Naumann et al., 2011). The native and treated proteinases were analyzed by SDS-PAGE under reducing conditions.

## 2.11. Functional characterization

### 2.11.1. Activity on plasma proteins, fibrinogen, fibrin, fibronectin and vitronectin

Human fibrinogen, fibrin and fibronectin were incubated with rhomb-I in a 1:200 (w/w) ratio at 37 °C in 50 mM Tris-HCl, 1 mM CaCl<sub>2</sub>, pH 8.0. In the case of vitronectin incubation with enzyme was in a ratio of 1:150. At various time intervals, 10 µl aliquots were analyzed by 12% SDS-PAGE under reducing conditions, and degradation products were visualized with Coomassie brilliant blue staining.

### 2.11.2. Proteolysis of matrigel

Matrigel Matrix (Corning, Bedford, MA, USA) was used to assess the effect of rhomb-I on BM components. Matrigel is a solubilized BM-like composite from Engelbreth-Holm-Swarm sarcoma, which is used as a surrogate of BM (Lebleu et al., 2007). Its main components are type-IV collagen, laminin, nidogen, and heparan sulfate proteoglycans. Matrigel (50 µg) was incubated with rhomb-I (1 µg) in 50 µl of 25 mM Tris-HCl, 150 mM NaCl, 2 mM CaCl<sub>2</sub>, pH 8.0 at 37 °C in the absence or presence of 10 mM EDTA. Aliquots were analyzed after 60 min by SDS-PAGE (7–15%) polyacrylamide gel under reducing conditions. Reactions were stopped by the addition of one volume of SDS-PAGE buffer (reducing conditions). The Matrigel compounds and their cleavage fragments were electro-transferred to a nitrocellulose membrane, analyzed by immunoblotting, and detected with specific antibodies against laminin (NB300-144, Novus, 1:5000), collagen-IV (70R31139, Fitzgerald, 1:4000) and nidogen (AF2570, RD Systems, 1:5000) (primary antibodies), and peroxidase-coupled protein G (diluted 1:5000) by chemiluminescence imaging system ChemiDoc.

### 2.11.3. Effect on platelet aggregation

To assess the effect of rhomb-I on platelet aggregation, human platelet suspension was prepared from the blood of consenting aspirin-free healthy volunteers. Venous blood was collected in acid-citrate dextrose (ACD: 78 mM citric acid; 117 mM sodium citrate; 282 mM dextrose) [6:1, (v/v)] centrifuged at 800×g for 15 min to obtain platelet-rich plasma (PRP). Human-washed platelets (WPs) were isolated as described previously (Sanchez et al., 2016). WPs were re-suspended in Tyrode's solution and adjusted to about  $2.5 \times 10^5$  platelets/µl. Platelet aggregation assays were monitored by light transmission in an eight channel platelet aggregometer (AggRam Helena Laboratories, Beaumont, TX, USA) with stirring at 600 rpm at 37 °C. To analyze the effect of rhomb-I on platelets, WPs (225 µl) or PRP were pre-incubated with the proteinase at different concentrations (WPs: 0.07–1.2 µM; PRP: 0.3–2.4 µM) in Tyrode's solution pH 7.4, 3 min. Platelets were stimulated by addition of several agonists: 10 µg/ml type I collagen, 10 µM ADP, 50 µg convulxin, 5.5 µg/ml vWF plus 0.5 mg/ml ristocetin. Ethical approval was granted by the FUNED human Ethics Committee (Protocol number: 35329520.4.00009507).

### 2.11.4. Effects of rhomb-I on commercial vWF and its recombinant A1 domain

To investigate the effect of the proteinase on vWF, 4 µg of vWF was incubated with rhomb-I (1 µg) for 60 min at 37 °C in phosphate buffered saline (PBS), pH 7.4. The reaction was stopped by the addition of sample buffer (8 M urea, 4% SDS, 4% 2-mercaptoethanol). Degradation products were analyzed by SDS-PAGE (7.5% gel). Recombinant vWF-A1 domain (rvWF-A1 domain, 10 µg) was incubated with or without enzyme (5 µg) for 60 min at 37 °C. Digestion was terminated with 5 µl of 10 mM EDTA. Aliquots were analyzed by SDS-PAGE (12.5% gel). The gels were either directly stained with Coomassie brilliant blue or transferred onto the nitrocellulose membrane. After blocking with 1% bovine serum albumin (BSA) in Tris-buffered saline 1 h, blots were developed with anti-mouse-rvWF-A1 domain IgG (1:400) and protein G peroxidase conjugated (Sigma-Aldrich) (1:3000) in subsequent incubation steps and, analyzed by chemiluminescence imaging system ChemiDoc.

### 2.11.5. Analysis of binding to and cleavage the platelet membrane receptors GPIIbα and GPVI

We have analyzed the interaction between rhomb-I and GPIIbα or GPVI from the membrane of WPs in response to rhomb-I. WPs ( $5 \times 10^5$  platelets/µl) were incubated in the absence or presence of 10 mM NEM (N-ethylmaleimide, Sigma) as a positive control, 100 nM GI254023X (inhibitor of ADAM10, Sigma), Co<sup>2+</sup> (10 mM) without or with rhomb-I (2 µg) at 37 °C for 60 min. Reactions were terminated by incubation for 5 min, 4 °C and then centrifuging at 1500×g for 2.5 min. To determine the interaction between rhomb-I and GPIIbα as well as the degradation and shedding of GPVI, Western blot assays were performed using specific antibodies as described recently (Sanchez et al., 2021).

## 3. Results and discussion

### 3.1. Purification and biochemical properties

The venom of the Atlantic bushmaster, *L. m. rhombeata* is rich in proteins/peptides that strongly affect hemostasis by activating or inhibiting platelet aggregation, coagulation, fibrinolysis, and thrombosis. In this study, its venom was size-fractionated by a gel filtration chromatography on Sephacryl S-200 into eight fractions (Fig. 1A). Fractions that exhibited either hemorrhagic or proteolytic activity were distributed mainly in fractions 2 and 5. The fraction 2 (tubes 70–79), which contained the main hemorrhagic SVMP of class P-III (approximately 55 kDa) is presently under investigation. We focused our attention on fraction 5 (tubes 100–110), which contained the protein of interest of approximately 23-kDa, exhibiting low hemorrhagic activity in mice and high proteolytic activity on DMC. The separation of fraction 5 on a Sephadex G-50 fine column under conditions described in Experimental methods, showed one peak with constant specific DMC proteolysis across the peak (Fig. 1B) and a low hemorrhagic effect (not shown). The homogeneity of this protein was established by two methods. First, one protein peak was observed by reverse phase HPLC on a C4 column (Fig. 1C). Second, this preparation gave a single protein band of approximately 23-kDa on SDS-PAGE under reducing and non-reducing conditions (Fig. 1C, inset). Analysis by MALDI-TOF mass spectrometry showed a M of 22,860 Da (Fig. 1D). This value in comparison to the calculated mass of rhomb-I, from its amino acid sequence (22,577 Da) gave a difference of 284 Da. Considering that the analysis was performed in the Bruker Autoflex III\_Smart Beam (Maldi TOF-TOF) equipment, in linear mode, which has a resolution  $>5000$  m/Δm and mass accuracy  $<20$  ppm, this variation was expected. Based on its molecular mass and source (*L. m. rhombeata* venom), the isolated proteinase corresponds to P-I class SVMPs and was called rhomb-I. The final step resulted in 23.5 mg from 2160 mg protein of crude venom. Table 1 summarizes the purification procedure. Several SVMPs were previously isolated by a two-step procedure, e.g. barnettlysin-I from *B. barnetti*

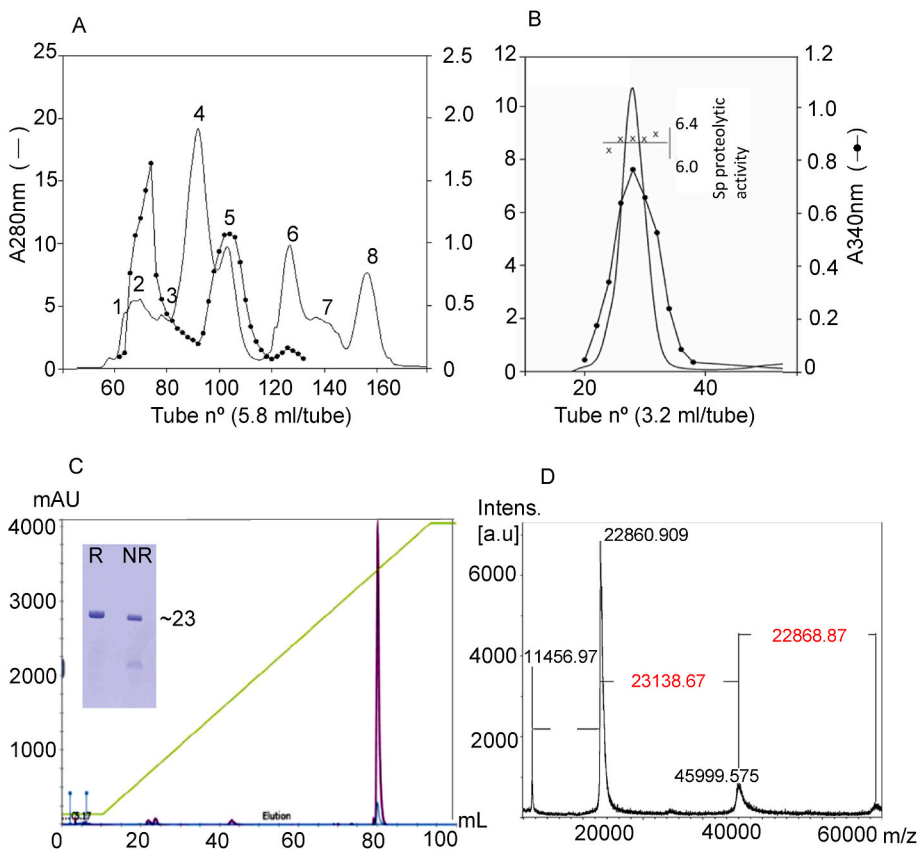


**Fig. 1.** Purification of rhomb-I. The isolation procedure is described in the purification section. Line, absorbance at 280 nm; filled circle, proteolytic activity on dimethylcasein, measured by absorbance at 340 nm. (A) Gel filtration on Sephacryl S-200, eluted with 0.05 M ammonium acetate buffer (pH 7.3) containing 0.3 M NaCl. (B) Gel filtration on Sephadex G-50 of the pooled active fraction 5 from the previous step, elution with 20 mM Hepes buffer, pH 7.5 containing 1 mM CaCl<sub>2</sub>. (C) RP-HPLC analysis of purified proteinase was performed using a Vydac C4 (250 × 4.6 mm) column. SDS-PAGE (12% gel) analysis of purified rhomb-I under reduced (R) or non-reduced (NR) conditions (inset). (D) Mass spectrometry of native rhomb-I. Purified rhomb-I was analyzed by MALDI-TOF/TOF. The main signal (displayed in arbitrary units – a.u.) represented a single ion charge of 22860.909 Da.

**Table 1**  
Purification of rhomb-I.

Step	Protein		Hemorrhagic activity					Proteolytic activity (DMC)			
	mg	%	MHD <sup>a</sup> (mg)	Specific activity <sup>b</sup> (U/mg. 10 <sup>3</sup> )	Total (U)	Yield %	PF	Specific activity <sup>c</sup> (U/mg)	Total (U)	Yield %	PF <sup>d</sup>
Crude venom	2160	100	0.005	0.0023	434.8	100	1	7.45	0.13	100	1
Sephacryl S-200	471.3	21.82	0.025	0.0144	69.4	20.13	4.9	21.4	0.047	36.1	2.9
Sephadex G-50	23.5	1.08	0.043	0.02	50	11.5	8.7	25.5	0.04	30.8	3.4

<sup>a</sup> Minimum Hemorrhagic Dose (MHD). One unit of hemorrhagic activity is one MHD.

<sup>b</sup> Specific activity is expressed as U/mg protein.

<sup>c</sup> One unit is defined as ΔA340/min.

<sup>d</sup> Purification Factor (PF).

(Sanchez et al., 2016). The progress of purification was followed by testing proteolysis on DMC (Estêvão-Costa et al., 2000), coagulant activity on Fg, fibrino (geno)lytic and amidolytic assays on DL-BAPNA (Magalhaes et al., 2003), and testing the in vivo hemorrhagic effect on each protein fraction. Likewise, hemorrhage caused by rhomb-I was similar to that inflicted by atroxlysin-I (atr-I, B. atrox), when injected (up to 50 μg) subcutaneously into mice, but different from the non-hemorrhagic SVMPs mut-II and leuc-a (Fig. 2A and B).

It is likely that some ions such as Ca<sup>2+</sup> and Mg<sup>2+</sup> have an important role in the stabilization of certain venom proteins, while others, particularly Zn<sup>2+</sup>, may actually participate in the catalysis of metalloenzymes. Thus, the effects of some cations on DMC degradation were examined. The addition of Ca<sup>2+</sup> and Mg<sup>2+</sup> (10 mM) enhanced rhomb-I proteolytic activity, whereas Zn<sup>2+</sup> and Co<sup>2+</sup> acted as effective inhibitors. Approximately 80% of the activity was lost in the presence of Co<sup>2+</sup>, and Zn<sup>2+</sup> ion (10 mM) completely blocked its activity (Fig. 2C). This result might be explained by the hypothesis that the metalloproteases have two Zn<sup>2+</sup>-binding sites: a stable structural zinc binding motif HEXGHXXGXXH and another zinc atom that together with calcium ions are required for the stability and expression of enzyme activity

(Nagase and Woessner, 1999; Oliveira et al., 2019). Similar data have been reported for other SVMPs (Bello et al., 2006; Oliveira et al., 2019) and MMPs (Nagase and Woessner, 1999). Like EDTA, the zinc binder inhibitors of MMPs: batimastat, marimastat, and the inhibitor of MMP-III (i-PIII), are effective blockers of rhomb-I activity. However, PMSF, an active-site serine protease inhibitor, had no effect (Fig. 2D). Furthermore, its catalytic function can be regulated by exchanging the cationic cofactor. The most abundant inhibitor of proteases found in plasma, α-2 macroglobulin (α-2M, 725-kDa), inhibits rhomb-I activity probably by physical entrapment as reported for other SVMPs (Sanchez et al., 2016). In vitro, the catalytic activity of rhomb-I decreased with increasing α-2M concentration and was eventually blocked completely at 1:1 α-2M stoichiometry of inhibitor/enzyme (Fig. 2E). Under reducing conditions, α-2M appeared as one main 180 kDa band corresponding to one of four equal subunits (Fig. 2F, lane C). The interaction of rhomb-I with α-2M was shown by 180 kDa subunit proteolysis to yield the characteristic 90 kDa band. Probably it was caused by the cleavage of the Arg<sup>696</sup>-Leu<sup>697</sup> bond, as identified for other P-I SVMPs such as barnettlysin-I (Sanchez et al., 2016) and leucurolysin-a (Bello et al., 2006), using as a model substrate: <sup>693</sup>GHARLVHVEEPH<sup>704</sup> that occurs at

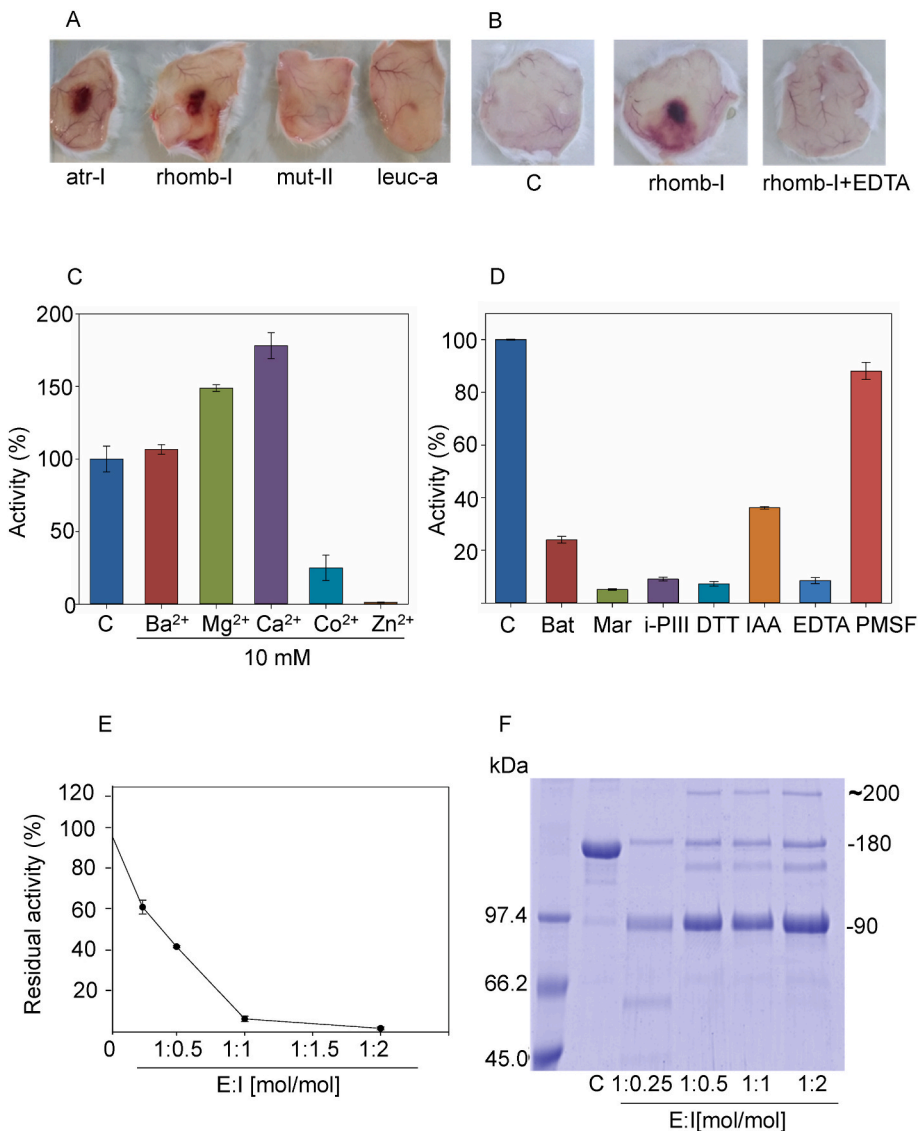


**Fig. 2.** Hemorrhage induced by P-I SVMPs. Subcutaneous injection (50  $\mu$ g) of each proteinase. In (A), atr-I and rhomb-I are hemorrhagic; mut-II and leuc-a are non-hemorrhagic, in (B), C (control saline), rhomb-I (50  $\mu$ g) and EDTA-treated rhomb-I. The dorsal skin of mice were removed after 4 h. In (C) effect of divalent cations and in (D) proteinase inhibitors on DMC proteolysis of rhomb-I. Rhomb-I (1  $\mu$ g) was incubated with each reagent as described in Experimental procedures, batimastat, marimastat, MMP-III inhibitor (0.5  $\mu$ M each), DTT (2 mM), IAA (1 mM), EDTA and PMSF (5 mM each). The remaining activity was assayed with DMC as substrate: C, control (enzyme only). In (E), Stoichiometry of inhibition of rhomb-I by  $\alpha$ 2-M. Rhomb-I (1  $\mu$ g) was incubated with various amounts of  $\alpha$ 2-M at molar ratios indicated on the abscissa [ $\alpha$ 2-M:enzyme = 0.25 to 2]. Residual proteinase activity in the mixture was tested with DMC, the ordinate indicates the remaining activity of rhomb-I as a percent of the original activity. In (F), Reduced SDS-PAGE (7.5%) profile of rhomb-I treated with  $\alpha$ 2-M. Molar ratios of  $\alpha$ 2-M:rhomb-I were 0.25–2. From top to bottom: The band at  $\sim$ 200-kDa may represent a complex of 180-kDa  $\alpha$ 2-M subunit with rhomb-I, the main cleavage fragment of  $\sim$ 90-kDa. C,  $\alpha$ 2-M control.

the bait region of  $\alpha$ 2-M. Also, the peptide: <sup>406</sup>RREYHTEKLVTSKGD<sup>420</sup> corresponding to  $\alpha$ -chain Fg was cleaved at K<sup>413</sup>-L<sup>414</sup> bond by the latter and other P-I SVMPs. The band of approximately 200 kDa may be the complex of  $\alpha$ 2-M/rhomb-I (Fig. 2F). In addition, rhomb-I underwent autoproteolysis yielding 20- and 11 kDa fragments as evidenced by SDS-PAGE (Fig. 1S, A, supplemental). In connection with these data Western blot analysis using rabbit-anti mut-II IgG reacted with these autoproteolytic fragments (Fig. 1S, B; mut-II is homologous P-I SVMP). Furthermore, direct sequence analysis of the N-terminal of the 11 kDa fragment of rhomb-I (Fig. 1S, A) provided YNGNLNTIRT sequence, that is identical to the rhomb-I sequence at position Y20 to T29 (Fig. 3, underlined). Also, the sequence NSVGIVQDHSPTK at position N118 to T130 has been determined from the same 11 kDa fragment (Fig. 3, underlined). A short sequence KPQCILNKP obtained from the sequence of the 20 kDa fragment is located in the C-terminal sequence of rhomb-I at position K193 to P201 (Fig. 3, underlined). In relation to these results, autoproteolysis has been described for other active SVMPs e.g. crotalin from *Crotalus atrox* (Wu et al., 2001) and brevilysin H6 from *Glodius halys brevicaudatus* (Fujimura et al., 2000) among others.

### 3.2. Structural characterization of rhomb-I

MS/MS spectra analysis of a tryptic digest of the purified rhomb-I

yielded fifteen peptides with homology to SVMPs sequence. A database searches identified these fragments as presented in Table 2S (Supplemental), as well as additional information for the peptide fragments identified by mass spectrometry. The protein sequence data for rhomb-I will appear in the UniProt database under the accession number COHM67. Multiple sequence alignment of mature rhomb-I with other SVMP sequences share a high percentage of identity (Fig. 3). As observed the protease domain presented a C-terminally extended zinc-binding motif, HEXXHXXGXXHD, with a hall-mark glycine and a third zinc-binding histidine or aspartate, and a conserved methionine which forms a unique “Met-turn” structure. These results confirm that rhomb-I belongs to P-I class SVMPs. Alignment between rhomb-I with LHF-II (P22796, *L.m.muta*) shows few differences in some residues at positions, 47–49, 53 and 70 (highlight in cyan). As shown in Fig. 3, rhomb-I lacks the N-linked glycosylation site (N-X-S/T) that has Ala 70, while LHF-II has Asn at the same position. The change of Asn by Ala in rhomb-I lead to the loss of a potential N-glycosylation site, thereby treatment rhomb-I with PNGase F did not affect the mobility of the proteinase (Fig. 1S, C).

### 3.3. Three dimensional model

The theoretical three-dimensional structure of rhomb-I (Fig. 4A–D)

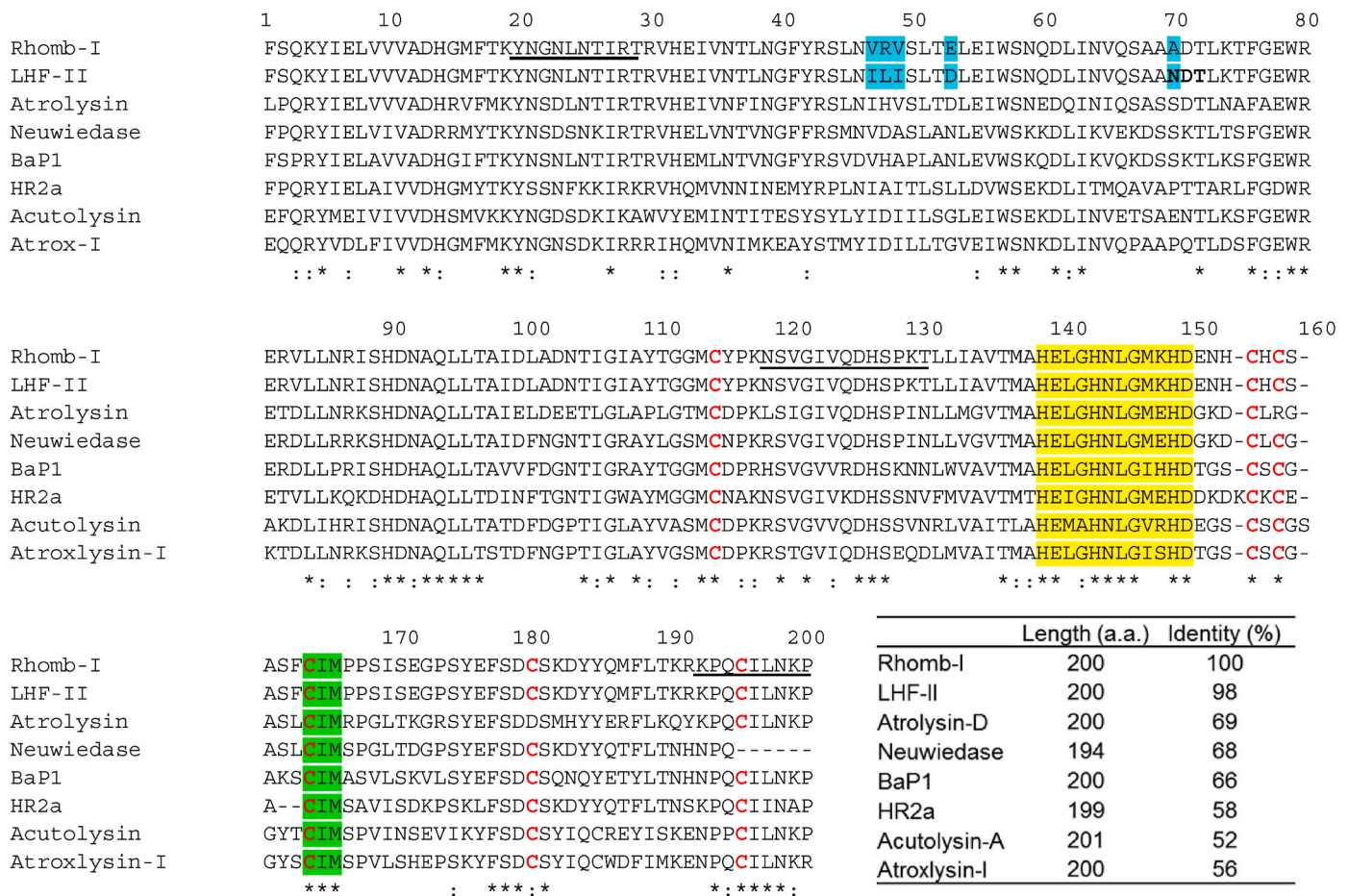


**Fig. 3.** Alignment of mature protein sequences of rhomb-I with others P-I SVMPs. The GenBank accession number of the sequences used are: LHF-II from *Lachesis muta muta* (P22796), atrolysin from *Crotalus atrox* (P15167), neuwiedase from *Bothrops pauloensis* (Q9I9R4), BaP1 from *Bothrops asper* (P83512), HR2a from *Protobothrops flavoviridis* (P14530), acutolysin-A from *Deinagkistrodon acutus* (Q9PW35) and atroxlysin-I from *Bothrops atrox* (P85420). (\*) identical residues; (.) strongly similar residues; (-) indicate gaps inserted to optimize the sequence identity. The zinc-binding motif and the methionine 165 of the characteristic basement Met-turn, are invariant and highlighted in yellow and green, respectively. The Cysteine residues are bold and highlighted in red. The sequences of the autocatalytic fragments of the 11-kDa: YNGNLNTIRT, NSVGIVQDHSPKT and a short sequence KPQCILNKP of the 20-kDa are underlined. Few differences in amino acid residues of rhomb-I with LHF-II at positions 47–49, 53 and 70 are highlighted in cyan. a.a., amino acids. Sequences were aligned using the CLUSTAL W Program. (For interpretation of the references to colour in this figure legend, the reader is referred to the Web version of this article.)

was predicted by the homology modeling (Šali and Blundell, 1993) using as templates: 3GBO (*B. moojeni*), 1DTH (*C. atrox*), 4AIG (*C. adamantus*), 4Q1L (*B. leucurus*) and 1ND1 (*B. asper*). Appropriate rhomb-I model was generated with Modeller v9.16 (Fiser and Šali, 2003). Analysis of the metal binding sites indicated that the theoretical architecture presents sites for Ca<sup>2+</sup> and Zn<sup>2+</sup> binding and are in homology with the used templates. A calcium ion is located on the surface of rhomb-I close to the C-terminus opposite to the catalytic site (Fig. 4B). It is known that catalytic activity of SVMPs depends on the protonation of the zinc-coordinating histidine residues on one hand and on the polarization capacity of the glutamate residue on the other.

### 3.4. Hydrolysis of plasma and ECM components

Hemorrhage is caused by proteolytic degradation of ECM components of blood vessels and coagulation-relevant serum proteins. Therefore, we assessed the enzymatic effects of rhomb-I on Fg, Fb, FN, VT, and Matrigel. Our data showed that rhomb-I is an α-fibrin (ogen)ase, as the α-chains of Fg and Fb were degraded within 5 and 20 min, respectively, without apparent effect on the β- and γ-chains (Fig. 5A and B). As shown in Fig. 5C, plasma FN was degraded to ~88 kDa band at 0.5 h, with the appearance of three additional fragments of ~59, ~133, and ~148 kDa after 3 h. Similarly, VT was hydrolyzed to a ~53, ~35 and ~25-kDa

products after 1 h incubation (Fig. 5D). To investigate the effect of rhomb-I on several BM proteins, Matrigel was incubated with the enzyme (60 min at 37 °C), and the extent of hydrolysis was analyzed on SDS-PAGE and confirmed by Western blot. Thus, Matrigel was digested into six main products of ~95, ~68, ~61 and ~43 kDa, concomitant with the reduction in the intensity of the protein bands of ~300- and 200 kDa of control (Fig. 6A, lane 1). Conversely, EDTA-treatment of rhomb-I completely abolished its activity (Fig. 6A, lane 2). These results were further analyzed by Western blot with specific antibodies against laminin (LM), type IV collagen, and nidogen (ND). Immunodetection of LM in Matrigel samples with anti-laminin revealed two main protein bands of ~300 and ~200 kDa (C, control sample), likely to representing to LM α1 and β1/γ1 chains, respectively. Rhomb-I cleaved LM chains into fragments of ~101, ~72, and ~56 kDa (Fig. 6B). Likewise, collagen IV, that run as uncleaved band of ~190 kDa (control coll-IV), is degraded into ~55, and ~30 kDa fragments (Fig. 6C). Nidogen antibodies revealed two main bands of ~151, and ~135 kDa (control ND). Under our experimental conditions, the band of ~151 kDa was completely digested, and three fragments of ~130-, ~65 and ~55 kDa were observed (Fig. 6D). Therefore, the results revealed that rhomb-I degrades the main proteins of BM in microvessels. Previous studies with the P-I SVMPs BaP1 from *B. asper* showed similar results, in comparison with a non-hemorrhagic leuc-a (*B. leucurus*) (Escalante

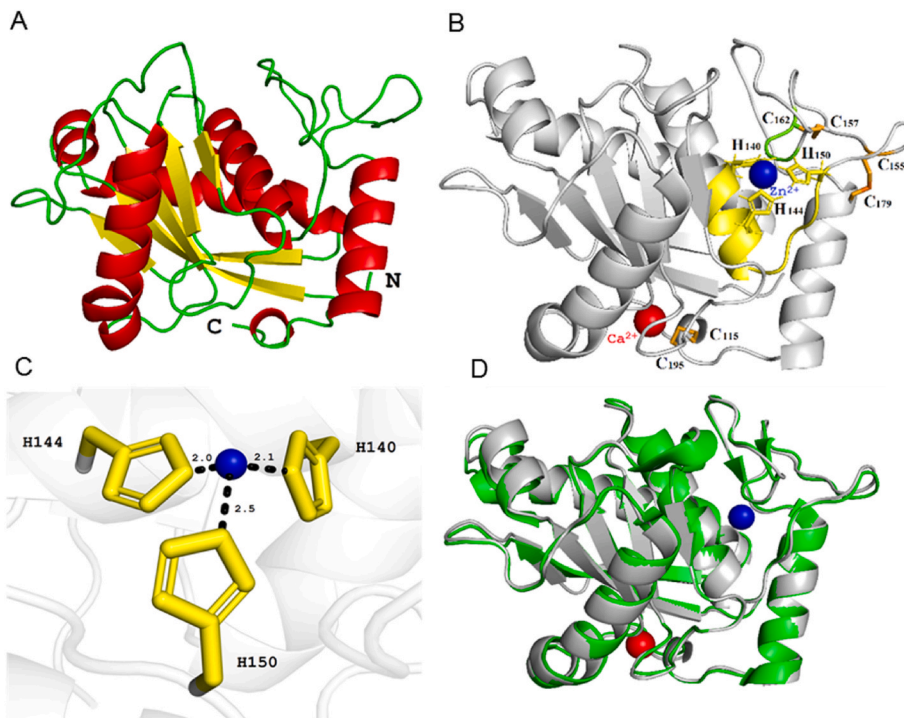


**Fig. 4.** 3D model of rhomb-I. (A) Final theoretical rhomb-I cartoon model showing alpha helix (red), beta sheet (yellow) and random coil (green); N and C: N-terminal and C-terminal respectively. (B) Functional motif; The conserved zinc binding motif and the met-turn are highlighted in yellow and bright green, respectively. The disulfide bridges are highlighted in orange, the Zn (blue sphere) and Ca (red sphere) cations are shown. (C) Zinc binding motif showing the coordination geometry between histidine residues in the active site and zinc ion is shown as in (B). The interactions are shown in black dashes. (D) Superposition of alpha C of rhomb-I (grey) with the structure of non-hemorrhagic metalloproteinase BmoomPa-I (PDB: 3GBO). The 3D model was generated by the homology criterion with the Modeller v 9.16 program and using five P-III SVMPS-III as templates (3GBO, 1DTH, 4AIG, 4Q1L and 1ND1). The PyMol program was used to visualise the structure. (For interpretation of the references to colour in this figure legend, the reader is referred to the Web version of this article.)

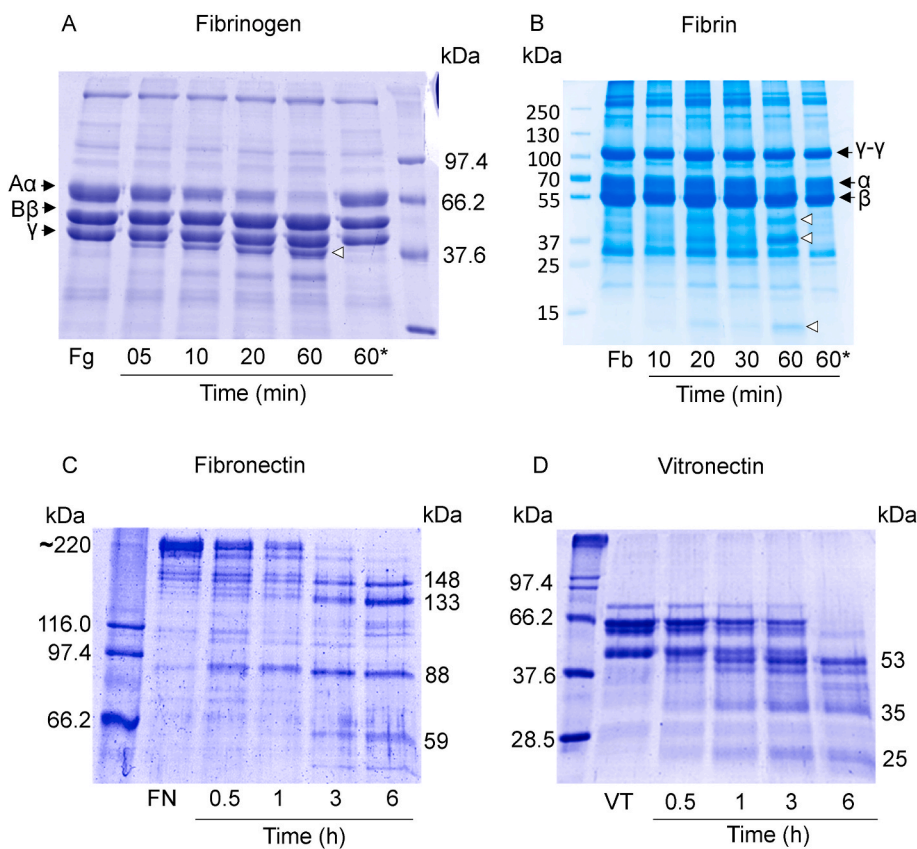


**Fig. 5.** Proteolysis of isolated plasma proteins by rhomb-I. Reducing SDS-PAGE (12.5% gel) of fibrinogen (Fig. A), fibrin (Fb, B), fibronectin (FN, C) and vitronectin (VT, D) after incubation with rhomb-I at the indicated intervals at 37 °C, at molar ratios of enzyme:substrate of 1:200 for Fg, Fb and FN, and 1:150 for VT. In controls, Fg and Fb were incubated for 60 min or 6 h (FN and VN) without rhomb-I. The reactions were stopped with reduced sample buffer. The polypeptide chains of fibrinogen and fibrin are indicated by black arrow heads. (\*) In (A) and (B) rhomb-I was pre-incubated with EDTA (5 mM) for 15 min before the reaction with Fg/Fb. The hydrolysis products are indicated by open arrow heads. In (C) and (D) the main digested products of FN and VT are indicated at the right.

et al., 2011). In this context, rhomb-I probably plays an important role in the rapid tissue damage observed in patients after bites from bushmaster snakes. Moreover, interesting insights to explain the action of P-III SVMPS in comparison with some P-I class underscore the complexity of

the pathology triggered by SVMPS in the microvasculature (Herrera et al., 2016).



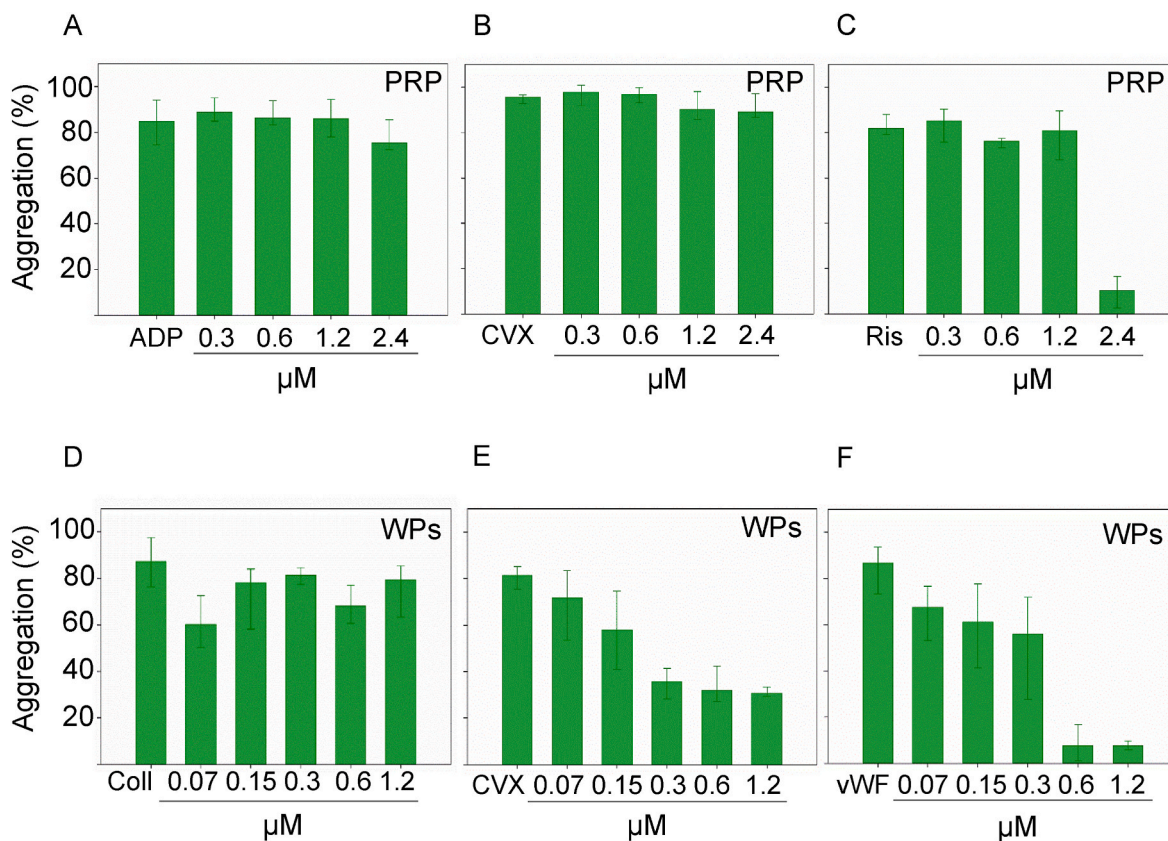


**Fig. 7.** Effect of rhomb-I on platelet aggregation of PRP and washed platelets (WPs). PRP (225  $\mu\text{L}$ ) or WPs (225  $\mu\text{L}$ ,  $2.5 \times 10^5/\mu\text{L}$ ) were pre incubated with rhomb-I at variable concentrations (0.3–4.8  $\mu\text{M}$  using PRP or 0.07–1.2  $\mu\text{M}$  with WPs), for 3 min under stirring at 600 rpm at 37  $^\circ\text{C}$ , before addition agonists to elicit aggregation; (A) ADP (10  $\mu\text{M}$ ), (B) convulxin (CVX, 50  $\mu\text{g}$ ), (C) ristocetin (Ris, 0.5 mg/ml), (D) collagen-I (10  $\mu\text{g}/\text{ml}$ ), (E) CVX (50  $\mu\text{g}$ ) and (F) vWF (5.5  $\mu\text{g}/\text{ml}$ ) plus Ris (0.5 mg/ml). Mean  $\pm$  standard deviation are shown. Rhomb-I inhibits aggregation of platelets in PRP triggered by Ris at concentration above 2.4  $\mu\text{M}$ . Also, rhomb-I blocks aggregation of WPs stimulated with CVX and vWF, with an  $\text{IC}_{50}$  values of 0.29  $\mu\text{M}$  and 0.21  $\mu\text{M}$ , respectively. Data are presented as percentage of control and are mean  $\pm$  standard deviation.

to vWF-A1 domain (~35 kDa), as shown by reduced SDS-PAGE and proved by Western blot with anti-mouse-rvWF-A1 domain-IgG (Fig. 8B). Furthermore, a band of ~27 kDa appeared after incubation of rvWF-A1-domain (~35 kDa) with rhomb-I, as observed by reduced SDS-PAGE and proved by immunoblotting assay (Fig. 8B, left and right panel). Under similar experimental conditions, differences were detected between P-I SVMPs: rhomb-I (hemorrhagic) and a non-hemorrhagic, mut-II, the last proteinase exhibited low cleavage rates on vWF, and on rvWF-A1-domain (Sanchez et al., 2021). Therefore, we analyzed the properties of vWF-GPIIb/IIIa axis after rhomb-I incubation of platelets at 37  $^\circ\text{C}$ . To this end, a platelet lysate was separated by SDS-PAGE and assayed for GPIIb/IIIa fragments by Western blot with CD42b/GPIIb/IIIa-antibody. Intact GPIIb/IIIa (140 kDa) was cleaved by rhomb-I to release two soluble products of ~130 kDa (glycocalicin) and ~35 kDa which were observed in total cell lysates and in supernatants as revealed by immunoblot with anti-human CD42b/GPIIb/IIIa-antibody (Fig. 8C, upper and lower panel). The band of ~35 kDa was also detected by homologous non-hemorrhagic SVMP kistomin, and suggests that the metalloproteinase cleaved GPVI near the mucin-like region (Hsu et al., 2008). Moreover, a band of ~45 kDa was released by endogenous metalloproteinases (ADAMs), but not by SVMP rhomb-I. The reason for this discrepancy remains to be elucidated. On the other hand, the collagen receptor GPVI was cleaved primarily by ADAM10, to shed a soluble ~55 kDa ectodomain (sGPVI) and a ~10 kDa cytoplasmic domain product. Incubation of platelet lysate with rhomb-I resulted in the release of a soluble 55 kDa and an additional band of ~45 kDa. The ~45 kDa fragment was not released by endogenous ADAM10 (Fig. 8D). In addition,  $\text{Co}^{2+}$ -treated rhomb-I reduced the shed of soluble forms of the two

receptors (Fig. 8 C and D). In connection with this, the antiplatelet properties of rhomb-I are similar to other SVMPs, e.g. mut-II which acts by shedding GPVI (Sanchez et al., 2021). However, the platelet-inhibiting effects via proteolytic cleavage of GPIIb/IIIa and GPVI may not distinguish between hemorrhagic (rhomb-I) and non-hemorrhagic P-I SVMPs (e.g. mut-II). This hypothesis merits further investigation. Low levels of GPVI, caused by deficiency or disease, enhance ADAM10-mediated shedding together with elevated plasma sGPVI, and is associated with a high risk of bleeding (Montague et al., 2018) as characterized by the pathology of snakebite envenoming by bushmaster and other vipers (Souza et al., 2007; Montague et al., 2018). It has been speculated that the physiological role of shedding is to limit platelet activation in intact vessels, mainly under high shear (Rayes et al., 2019). To test this hypothesis, rhomb-I (5  $\mu\text{g}$ ) was added to WPs (15  $\mu\text{L}$ ) for 30 min at 37  $^\circ\text{C}$ , then subjected to SDS-PAGE (7–15% gel) and electroblotted onto a nitrocellulose membrane. Thereafter, platelet lysates and supernatants were immunoblotted with anti-GPIIb/IIIa-antibody or anti-GPVI antibody. As shown in Fig. 8E, rhomb-I strongly bound to both platelet receptors (Fig. 8E, left and right panel). Taken together these results indicate that rhomb-I binds to and cleaves GPIIb/IIIa and GPVI.

#### 4. Conclusions

This study provides important structural and biological properties of the metalloproteinase rhomb-I from *L. m. rhombeata* venom, which strongly affects vWF, essential for hemostasis, and the platelet receptors, GPIIb/IIIa and GPVI, thereby affecting vascular permeability and platelet aggregation. In addition, rhomb-I contributes to toxicity through local

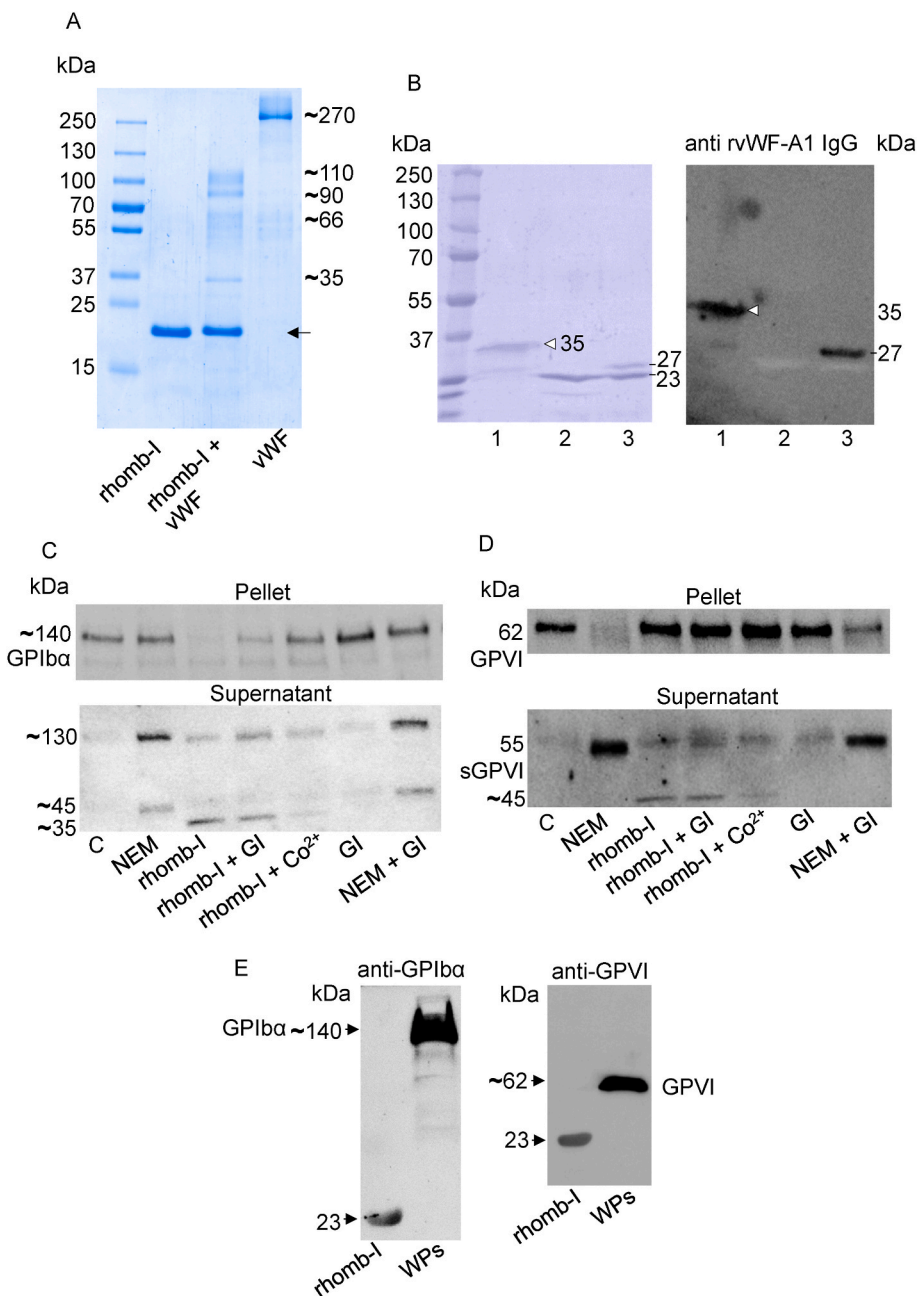


**Fig. 8.** Antiplatelet effect of rhomb-I assay by immunoblotting upon commercial vWF, its recombinant A1 domain and platelet surface glycoproteins (GPIIb and GPVI). (A) Cleavage of vWF (4 µg) after incubation with rhomb-I (1 µg). Degradation fragments were analyzed by SDS-PAGE (7.5% gel) under reducing conditions. Controls, rhomb-I and commercial vWF (~270 kDa) are shown. (B) rvWF-A1 domain (10 µg) incubated with rhomb-I (5 µg) were subjected to SDS PAGE (12.5% gel) under reducing conditions followed by immunoblotting with anti-rvWF-A1 domain antibody recognizing the rvWF-A1 domain (open arrow head, ~35-kDa) and a product of ~27-kDa. The band of 23-kDa is rhomb-I (lane 2 and 3 in B). (C) Immunoblot with anti-GPIIb antibody or (D) with anti-GPVI antibody of platelets pellet or supernatant of washed platelets ( $5 \times 10^5/\mu\text{L}$ ) treated with: NEM (0.1 mM), rhomb-I (2 µg), rhomb-I plus GI254023X (GI, 100 nM), rhomb-I plus  $\text{Co}^{2+}$  (10 mM), GI254023X (GI, 100 nM), and NEM (0.1 mM) plus GI254023X (GI, 100 nM). (E) rhomb-I binds to the receptors GPIIb and GPVI, rhomb-I (5 µg) were added in 15 µl of WPs ( $5 \times 10^5/\mu\text{L}$ ). The reactions were stopped with sample buffer (1:1, v/v) and boiling for 5 min. WPs without treatment were used as positive control. The samples were subjected to SDS-PAGE (7.5–15%), transferred to nitrocellulose membrane followed by immunoblotting with anti-GPIIb or anti-GPVI antibodies. Each experiment in panels B, C, D and E is representative of four similar experiments.

damage and, more importantly, systemic changes. These include hemorrhage and consumption-induced coagulopathy, cardiovascular collapse and autonomic nervous system changes caused by bushmaster venom directly or indirectly related to SVMPs. Even more difficult is understanding the detailed molecular determinants of protein-protein binding of SVMPs to induce severe bleeding, which remains elusive.

#### Credit authors statement

EFS, VGA, LSO, GOS, DVR, designed the study and performed experiments; EFS, AMMS, VGA, RS, MHB, DVR, JAE, conceptualization, resources, analyzed and interpreted data, EFS; writing-original draft preparation, EFS, AMMS and JAE; writing-review and editing. All the authors contributed equally to the draft revisions and approved the manuscript.

#### Funding

This work was supported by Brazilian Agencies: Fundação de Amparo a Pesquisa do Estado de Minas Gerais (FAPEMIG, grant # APQ-01724-18), Conselho Nacional de Desenvolvimento Científico e Tecnológico (CNPq, grants #: 301,326/2018–5, 309,823–8), Programa Nacional de Investigación Científica y Estudios Avanzados (PROCIENCIA: grant 079-2021-FONDECYT). VGA is a recipient of CAPES, grant # 88882442320/19. EFS and AMMS are recipients of CNPq-PQ. JAE is financially supported by the German Research Foundation (DFG – Project-ID, 194468054 – SFB 1009 project A09) and by the Interdisciplinary Center of Clinical Research (IZKF grant: Ebl-A/009/21). This study is part of the PhD Thesis of VGA at Science-Toxinology Course of Butantan Institute, SP.

## Ethical statement

Authors declarer that the data contained in this study are original.

## Declaration of competing interest

The authors declare that they have no known competing financial interests or personal relationships that could have appeared to influence the work reported in this paper.

## Data availability

Data will be made available on request.

## Acknowledgements

The authors would like to thank Prof. Solange M. T. Serrano, Butantan Institute for MS/Ms analysis of rhomb-I autoproteolytic fragments.

## Appendix B. Supplementary data

Supplementary data to this article can be found online at <https://doi.org/10.1016/j.toxicon.2023.107097>.

## References

- Andrews, R.K., Karunakaran, D., Gardiner, E.E., Berndt, M.C., 2007. Platelet receptor proteolysis: a mechanism for downregulating platelet reactivity. *Arterioscler. Thromb. Vasc. Biol.* 27 (7), 1511–1520. <https://doi.org/10.1161/ATVBAHA.107.141390>.
- Bello, C.A., Hermogenes, A.L.N., Magalhaes, A., Veiga, S.S., Gremski, L.H., Richardson, M., Sanchez, E.F., 2006. Isolation and biochemical characterization of a fibrinolytic proteinase from *Bothrops leucurus* (White-tailed jararaca) snake venom. *Biochimie* 88 (2), 189–200. <https://doi.org/10.1016/j.biochi.2005.07.008>.
- Brust, A., Sunagar, K., Undheim, E.A.B., Vetter, I., Yang, D.C., Casewell, N.R., Jackson, T. N.W., Koludarov, I., Alewood, P.F., Hodgson, W.C., Lewis, R.J., King, G.F., Antunes, A., Hendriks, I., Fry, B.G., 2013. Differential evolution and neofunctionalization of snake venom metalloprotease domains. *Mol. Cell. Proteomics* 12 (3), 651–663. <https://doi.org/10.1074/mcp.M112.023135>.
- Calvete, J.J., 2011. Proteomic tools against the neglected pathology of snake bite envenoming. *Expert Rev. Proteomics* 8 (6), 739–758. <https://doi.org/10.1586/epn.11.61>.
- Campbell, J.A., Lamar, W.W., 2004. *The Venomous Reptiles of the Western Hemisphere*. Comstock Pub. Associates.
- Casewell, N.R., Wagstaff, S.C., Harrison, R.A., Renjifo, C., Wuster, W., 2011. Domain loss facilitates accelerated evolution and neofunctionalization of duplicate snake venom metalloproteinase toxin genes. *Mol. Biol. Evol.* 28 (9), 2637–2649. <https://doi.org/10.1093/molbev/msr091>.
- Casewell, N.R., Wuster, W., Vonk, F.J., Harrison, R.A., Fry, B.G., 2013. Complex cocktails: the evolutionary novelty of venoms. *Trends Ecol. Evol.* 28 (4), 219–229. <https://doi.org/10.1016/j.tree.2012.10.020>.
- Chippaux, J.-P., 2017. Incidence and mortality due to snakebite in the Americas. *PLoS Neglected Trop. Dis.* 11 (6), e0005662. <https://doi.org/10.1371/journal.pntd.0005662>.
- Cordeiro, F.A., Coutinho, B.M., Wiesel, G.A., Bordon, K. de C.F., Bregge-Silva, C., Rosa-Garzon, N.G., Cabral, H., Ueberheide, B., Arantes, E.C., 2018. Purification and enzymatic characterization of a novel metalloprotease from *Lachesis muta rhombeata* snake venom. *J. Venom. Anim. Toxins Incl. Trop. Dis.* 24 (1), 32. <https://doi.org/10.1186/s40409-018-0171-x>.
- Damico, D.C.S., Bueno, L.G.F., Rodrigues-Simioni, L., Marangoni, S., da Cruz-Höfling, M. A., Novello, J.C., 2006. Functional characterization of a basic D49 phospholipase A2 (Lmxt-i) from the venom of the snake *Lachesis muta muta* (Bushmaster). *Toxicon* 47 (7), 759–765. <https://doi.org/10.1016/j.toxicon.2006.02.007>.
- Delano, W.S., 2002. The PyMOL Molecular Graphics System. De Lano Scientific, San Carlos, CA. <http://www.pymol.org>.
- Escalante, T., Ortiz, N., Rucavado, A., Sanchez, E.F., Richardson, M., Fox, J.W., Gutiérrez, J.M., 2011. Role of collagens and perlecan in microvascular stability: exploring the mechanism of capillary vessel damage by snake venom metalloproteinases. *PLoS One* 6 (12), e28017. <https://doi.org/10.1371/journal.pone.0028017>.
- Estevão-Costa, M.L., Diniz, C.R., Magalhães, A., Markland, F.S., Sanchez, E.F., 2000. Action of metalloproteinases mutalysin i and ii on several components of the hemostatic and fibrinolytic systems. *Thromb. Res.* 99 (4), 363–376. [https://doi.org/10.1016/S0049-3848\(00\)00259-0](https://doi.org/10.1016/S0049-3848(00)00259-0).
- Felicio, L.F., Souza, C.T., Velarde, D.T., Magalhaes, A., Almeida, A.P., Figueiredo, S., Richardson, M., Diniz, C.R., Sanchez, E.F., 2003. Kallikrein-like proteinase from bushmaster snake venom. *Protein Expr. Purif.* 30 (1), 32–42. [https://doi.org/10.1016/S1046-5928\(03\)00053-6](https://doi.org/10.1016/S1046-5928(03)00053-6).
- Fiser, A., Šali, A., 2003. Modeller: generation and refinement of homology-based protein structure models. *Methods Enzymol.* 374, 461–491. [https://doi.org/10.1016/S0076-6879\(03\)74020-8](https://doi.org/10.1016/S0076-6879(03)74020-8). Elsevier.
- Fox, J.W., Serrano, S.M.T., 2005. Structural considerations of the snake venom metalloproteinases, key members of the M12 reprolysin family of metalloproteinases. *Toxicon* 45 (8), 969–985. <https://doi.org/10.1016/j.toxicon.2005.02.012>.
- Fry, B.G., Scheib, H., van der Weerd, L., Young, B., McNaughtan, J., Ramjan, S.F.R., Vidal, N., Poelmann, R.E., Norman, J.A., 2008. Evolution of an arsenal. *Mol. Cell. Proteomics* 7 (2), 215–246. <https://doi.org/10.1074/mcp.M700094-MCP200>.
- Fujimura, S., Oshikawa, K., Terada, S., Kimoto, E., 2000. Primary structure and autoproteolysis of brevilysin h6 from the venom of *Gloydius halys brevicaudus*. *J. Biochem.* 128 (2), 167–173. <https://doi.org/10.1093/oxfordjournals.jbchem.a022737>.
- Fuly, A.L., Calil-Elias, S., Zingali, R.B., Guimarães, J.A., Melo, P.A., 2000. Myotoxic activity of an acidic phospholipase A2 isolated from *Lachesis muta* (Bushmaster) snake venom. *Toxicon* 38 (7), 961–972. [https://doi.org/10.1016/S0041-0101\(99\)00208-1](https://doi.org/10.1016/S0041-0101(99)00208-1).
- Gomis-Rüth, F.X., 2003. Structural aspects of the metzincin clan of metalloendopeptidases. *Mol. Biotechnol.* 24 (2), 157–202. <https://doi.org/10.1385/MB:24:2:157>.
- Grover, S.P., Bergmeier, W., Mackman, N., 2018. Platelet signaling pathways and new inhibitors. *Arterioscler. Thromb. Vasc. Biol.* 38 (4) <https://doi.org/10.1161/ATVBAHA.118.310224>.
- Herrera, C., Voisin, M.-B., Escalante, T., Rucavado, A., Nourshargh, S., Gutiérrez, J.M., 2016. Effects of PI and PIII snake venom haemorrhagic metalloproteinases on the microvasculature: a confocal microscopy study on the mouse cremaster muscle. *PLoS One* 11 (12), e0168643. <https://doi.org/10.1371/journal.pone.0168643>.
- Hsu, C.C., Wu, W.B., Huang, T.F., 2008. A snake venom metalloproteinase, kistomin, cleaves platelet glycoprotein VI and impairs platelet functions. *J. Thromb. Haemostasis*. <https://doi.org/10.1111/j.1538-7836.2008.03071.x>.
- Humphrey, W., Dalke, A., Schulten, K., 1996. VMD: visual molecular dynamics. *J. Mol. Graph.* 14 (1), 33–38. [https://doi.org/10.1016/0263-7855\(96\)00018-5](https://doi.org/10.1016/0263-7855(96)00018-5).
- Junqueira-de-Azevedo, I.L.M., Ching, A.T.C., Carvalho, E., Faria, F., Nishiyama, M.Y., Ho, P.L., Diniz, M.R.V., 2006. *Lachesis muta* (Viperidae) cDNAs reveal diverging pit viper molecules and scaffolds typical of cobra (Elapidae) venoms: implications for snake toxin repertoire evolution. *Genetics* 173 (2), 877–889. <https://doi.org/10.1534/genetics.106.056515>.
- Kini, R., Koh, C., 2016. Metalloproteases affecting blood coagulation, fibrinolysis and platelet aggregation from snake venoms: definition and nomenclature of interaction sites. *Toxins* 8 (10), 284. <https://doi.org/10.3390/toxins8100284>.
- Laemmli, U.K., 1970. Cleavage of structural proteins during the assembly of the head of bacteriophage t4. *Nature* 227 (5259), 680–685. <https://doi.org/10.1038/227680a0>.
- LeBleu, V.S., MacDonald, B., Kalluri, R., 2007. Structure and function of basement membranes. *Exp. Biol. Med.* 232 (9), 1121–1129. <https://doi.org/10.3181/0703-MR-72>.
- Madrigal, M., Sanz, L., Flores-Díaz, M., Sasa, M., Núñez, V., Alape-Girón, A., Calvete, J.J., 2012. Snake venomomics across genus *Lachesis*. Ontogenetic changes in the venom composition of *Lachesis stenophrys* and comparative proteomics of the venoms of adult *Lachesis melanocephala* and *Lachesis acrochorda*. *J. Proteomics* 77, 280–297. <https://doi.org/10.1016/j.jprot.2012.09.003>.
- Magalhaes, A., Ferreira, R.N., Richardson, M., Gontijo, S., Yarleque, A., Magalhaes, H.P. B., Bloch, C., Sanchez, E.F., 2003. Coagulant thrombin-like enzymes from the venoms of Brazilian and Peruvian bushmaster (*Lachesis muta muta*) snakes. *Comp. Biochem. Physiol. B Biochem. Mol. Biol.* 136 (2), 255–266. [https://doi.org/10.1016/S1096-4959\(03\)00202-1](https://doi.org/10.1016/S1096-4959(03)00202-1).
- Montague, S.J., Andrews, R.K., Gardiner, E.E., 2018. Mechanisms of receptor shedding in platelets. *Blood* 132 (24), 2535–2545. <https://doi.org/10.1182/blood-2018-03-742668>.
- Moura-da-Silva, A., Almeida, M., Portes-Junior, J., Nicolau, C., Gomes-Neto, F., Valente, R., 2016. Processing of snake venom metalloproteinases: generation of toxin diversity and enzyme inactivation. *Toxins* 8 (6), 183. <https://doi.org/10.3390/toxins8060183>.
- Moura-da-Silva, A.M., Theakston, R.D.G., Crampton, J.M., 1996. Evolution of disintegrin cysteine-rich and mammalian matrix-degrading metalloproteinases: gene duplication and divergence of a common ancestor rather than convergent evolution. *J. Mol. Evol.* 43 (3), 263–269. <https://doi.org/10.1007/BF02338834>.
- Nachtigall, P.G., Freitas-de-Sousa, L.A., Mason, A.J., Moura-da-Silva, A.M., Grazziotin, F. G., Junqueira-de-Azevedo, I.L.M., 2022. Differences in pla 2 constitution distinguish the venom of two endemic Brazilian mountain lanceheads, *Bothrops cotiara* and *Bothrops fonsecai*. *Toxins* 14 (4), 237. <https://doi.org/10.3390/toxins14040237>.
- Nagase, H., Woessner, J.F., 1999. Matrix metalloproteinases. *J. Biol. Chem.* 274 (31), 21491–21494. <https://doi.org/10.1074/jbc.274.31.21491>.
- Naumann, G.B., Silva, L.F., Silva, L., Faria, G., Richardson, M., Evangelista, K., Kohlhoff, M., Gontijo, C.M.F., Navdaev, A., de Rezende, F.F., Eble, J.A., Sanchez, E. F., 2011. Cytotoxicity and inhibition of platelet aggregation caused by an L-amino acid oxidase from *Bothrops leucurus* venom. *Biochim. Biophys. Acta, Gen. Subj.* 1810 (7), 683–694. <https://doi.org/10.1016/j.bbagen.2011.04.003>.
- Oliveira, L.S., Estevão-Costa, M.L., Alvarenga, V.G., Vivas-Ruiz, D.E., Yarleque, A., Lima, A.M., Cavaco, A., Eble, J.A., Sanchez, E.F., 2019. Atroxlysin-III, a metalloproteinase from the venom of the Peruvian pit viper snake *Bothrops atrox* (Jergón) induces glycoprotein VI shedding and impairs platelet function. *Molecules* 24 (19), 3489. <https://doi.org/10.3390/molecules24193489>.

- Pla, D., Sanz, L., Molina-Sánchez, P., Zorita, V., Madrigal, M., Flores-Díaz, M., Alape-Girón, A., Núñez, V., Andrés, V., Gutiérrez, J.M., Calvete, J.J., 2013. Snake venomomics of *Lachesis muta rhombata* and genus-wide antivenomics assessment of the paraspecific immunoreactivity of two antivenoms evidence the high compositional and immunological conservation across *Lachesis*. *J. Proteomics* 89, 112–123. <https://doi.org/10.1016/j.jprot.2013.05.028>.
- Polgár, J., Clemetson, J.M., Kehrel, B.E., Wiedemann, M., Magnenat, E.M., Wells, T.N.C., Clemetson, K.J., 1997. Platelet activation and signal transduction by convulxin, a c-type lectin from *Crotalus durissus terrificus* (Tropical rattlesnake) venom via the p62/GPVI collagen receptor. *J. Biol. Chem.* 272 (21), 13576–13583. <https://doi.org/10.1074/jbc.272.21.13576>.
- Rayes, J., Watson, S.P., Nieswandt, B., 2019. Functional significance of the platelet immune receptors GPVI and CLEC-2. *J. Clin. Invest.* 129 (1), 12–23. <https://doi.org/10.1172/JCI122955>.
- Šali, A., Blundell, T.L., 1993. Comparative protein modelling by satisfaction of spatial restraints. *J. Mol. Biol.* 234 (3), 779–815. <https://doi.org/10.1006/jmbi.1993.1626>.
- Sanchez, E.F., 2004. *Mutalysins*. In: Barret, A.J., Rawlings, N.D., Woessner, J.F. (Eds.), *Handbook of Proteolytic Enzymes*, second ed. Elsevier Ltd, pp. 32–42.
- Sanchez, E.F., Felicori, L.F., Chavez-Olortegui, C., Magalhaes, H.B.P., Hermogenes, A.L., Diniz, M.V., Junqueira-de-Azevedo, I. de L.M., Magalhaes, A., Richardson, M., 2006. Biochemical characterization and molecular cloning of a plasminogen activator proteinase (Lv-pa) from bushmaster snake venom. *Biochim. Biophys. Acta, Gen. Subj.* 1760 (12), 1762–1771. <https://doi.org/10.1016/j.bbagen.2006.08.023>.
- Sanchez, E.F., Freitas, T.V., Ferreira-Alves, D.L., Velarde, D.T., Diniz, M.R., Cordeiro, M. N., Agostini-Cotta, G., Diniz, C.R., 1992. Biological activities of venoms from South American snakes. *Toxicol* 30 (1), 95–103. [https://doi.org/10.1016/0041-0101\(92\)90505-Y](https://doi.org/10.1016/0041-0101(92)90505-Y).
- Sanchez, E.F., Richardson, M., Gremski, L.H., Veiga, S.S., Yarleque, A., Niland, S., Lima, A.M., Estevo-Costa, M.I., Eble, J.A., 2016. A novel fibrinolytic metalloproteinase, barnettysin-I from *Bothrops barnetti* (Barnett's pitviper) snake venom with anti-platelet properties. *Biochim. Biophys. Acta, Gen. Subj.* 1860 (3), 542–556. <https://doi.org/10.1016/j.bbagen.2015.12.021>.
- Sanchez, E.F., Santos, C.I., Magalhaes, A., Diniz, C.R., Figueiredo, S., Gilroy, J., Richardson, M., 2000. Isolation of a proteinase with plasminogen-activating activity from *Lachesis muta muta* (Bushmaster) snake venom. *Arch. Biochem. Biophys.* 378 (1), 131–141. <https://doi.org/10.1006/abbi.2000.1781>.
- Sanchez, E., Flores-Ortiz, R., Alvarenga, V., Eble, J., 2017. Direct fibrinolytic snake venom metalloproteinases affecting hemostasis: structural, biochemical features and therapeutic potential. *Toxins* 9 (12), 392. <https://doi.org/10.3390/toxins9120392>.
- Sanchez, Eladio F., Alvarenga, Valeria G., Oliveira, Luciana S., Oliveira, Débora L., Estevo-Costa, Maria I., Flores-Ortiz, R., Eble, Johannes A., 2021. A fibrinolytic snake venom metalloproteinase, mutalysin-II, with antiplatelet activity and targeting capability toward glycoprotein GPIIb and glycoprotein GPVI. *Biochimie* 184, 1–7. <https://doi.org/10.1016/j.biochi.2021.01.016>.
- Sanz, L., Escolano, J., Ferretti, M., Biscoglio, M.J., Rivera, E., Crescenti, E.J., Angulo, Y., Lomonte, B., Gutiérrez, J.M., Calvete, J.J., 2008. Snake venomomics of the South and Central American Bushmasters. Comparison of the toxin composition of *Lachesis muta* gathered from proteomic versus transcriptomic analysis. *J. Proteomics* 71 (1), 46–60. <https://doi.org/10.1016/j.jprot.2007.10.004>.
- Serrano, S.M.T., Shannon, J.D., Wang, D., Camargo, A.C.M., Fox, J.W., 2005. A multifaceted analysis of viperid snake venoms by two-dimensional gel electrophoresis: an approach to understanding venom proteomics. *Proteomics* 5 (2), 501–510. <https://doi.org/10.1002/prot.200400931>.
- Slagboom, J., Kool, J., Harrison, R.A., Casewell, N.R., 2017. Haemotoxic snake venoms: their functional activity, impact on snakebite victims and pharmaceutical promise. *Br. J. Haematol.* 177 (6), 947–959. <https://doi.org/10.1111/bjh.14591>.
- Souza, R.C.G., Nogueira, A.P.B., Lima, T., Cardoso, J.L.C., 2007. The enigma of the North margin of the Amazon River: proven *Lachesis* bites in Brazil, report of two cases, general considerations about the genus and bibliographic review. *Bull. Chic. Herpetol. Soc.* 42 (7), 105–115.
- Stephano, M.A., Guidolin, R., Higashi, H.G., Tambourgi, D.V., Sant'Anna, O.A., 2005. The improvement of the therapeutic anti-*Lachesis muta* serum production in horses. *Toxicol* 45 (4), 467–473. <https://doi.org/10.1016/j.toxicol.2004.12.006>.
- Takeda, S., 2016. ADAM and ADAMTS family proteins and snake venom metalloproteinases: a structural overview. *Toxins* 8 (5), 155. <https://doi.org/10.3390/toxins8050155>.
- Takeda, S., Igarashi, T., Mori, H., Araki, S., 2006. Crystal structures of VAP1 reveal ADAMs' MDC domain architecture and its unique C-shaped scaffold. *EMBO J.* 25 (11), 2388–2396. <https://doi.org/10.1038/sj.emboj.7601131>.
- Tanus Jorge, M., Sano-Martins, S., Tomy, I.C., Castro, S.C.B., S.A. Ferrari, R., Ribeiro, Adriano, L., A. Warrell, D., 1997. Snakebite by the bushmaster (*Lachesis muta*) in Brazil: case report and review of the literature. *Toxicol* 35 (4), 545–554. [https://doi.org/10.1016/S0140-6736\(95\)92825-1](https://doi.org/10.1016/S0140-6736(95)92825-1).
- Torres, R., Jaime, R., Torres, A., María, A., Arroyo-Parejo, Max, A., 1995. Coagulation disorders in bushmaster envenomation. *Lancet* 346 (8972), 449–450. [https://doi.org/10.1016/S0140-6736\(95\)92825-1](https://doi.org/10.1016/S0140-6736(95)92825-1).
- Vetter, I., Davis, J.L., Rash, L.D., Anangi, R., Mobli, M., Alewood, P.F., Lewis, R.J., King, G.F., 2011. Venomics: a new paradigm for natural products-based drug discovery. *Amino Acids* 40 (1), 15–28. <https://doi.org/10.1007/s00726-010-0516-4>.
- Vilahir, G., Gutiérrez, M., Arzanauskaitė, M., Mendieta, G., Ben-Aicha, S., Badimon, L., 2018. Intracellular platelet signalling as a target for drug development. *Vasc. Pharmacol.* 111, 22–25. <https://doi.org/10.1016/j.vph.2018.08.007>.
- Weinberg, M.L.D., Felicori, L.F., Bello, C.A., Magalhães, H.P.B., Almeida, A.P., Magalhães, A., Sanchez, E.F., 2004. Biochemical properties of a bushmaster snake venom serine proteinase (LV-KA), and its kinin releasing activity evaluated in rat mesenteric arterial rings. *J. Pharmacol. Sci.* 96 (3), 333–342. <https://doi.org/10.1254/jphs.FPJ04005X>.
- Whittaker, C.A., Hynes, R.O., 2002. Distribution and evolution of von willebrand/ integrin domains: widely dispersed domains with roles in cell adhesion and elsewhere. *Mol. Biol. Cell* 13 (10), 3369–3387. <https://doi.org/10.1091/mbc.02-05-0259>.
- Wiesel, G.A., Bordon, K.C., Silva, R.R., Gomes, M.S., Cabral, H., Rodrigues, V.M., Ueberheide, B., Arantes, E.C., 2019. Subproteome of *Lachesis muta rhombata* venom and preliminary studies on LmrSP-4, a novel snake venom serine proteinase. *J. Venom. Anim. Toxins Incl. Trop. Dis.* 25, e147018 <https://doi.org/10.1590/1678-9199-jvatitd-1470-18>.
- Wu, W.-B., Peng, H.-C., Huang, T.-F., 2001. Crotalin, a vWF and GP Ib cleaving metalloproteinase from venom of *Crotalus atrox*. *Thromb. Haemostasis* 86 (12), 1501–1511. <https://doi.org/10.1055/s-0037-1616755>.